Cureus Journal of Engineering

Open Access Original Article

Effect of Linear Thermal Expansion on Quasi-Thermoelastic Wave in an Incompressible Transversely Isotropy Based on Different Materials

Received 04/03/2025
Review began 04/11/2025
Review ended 05/05/2025
Published 05/30/2025

DOI: https://doi.org/10.7759/s44388-025-04469-0

R. Lianngenga [1] , Jongte Lalvohbika [2] , Fanai Lalhriattira [3] , T.B.C. Laldinnmawia [3]

1. Department of Mathematics, Government Champhai College, Champhai, IND 2. Department of Mathematics, Pachhunga University College, Aizawl, IND 3. Department of Mathematics and Computer Science, Mizoram University, Aizawl, IND

Corresponding author: R. Lianngenga, rengsi.9@gmail.com

Abstract

This paper investigated the propagation of quasi-thermoelastic waves at an incompressible transversely isotropic solid half-space and the effect of linear thermal expansion. In this material, we have observed the existence of two waves, quasi-primary wave *(qP)* and quasi-thermal wave *(qT)*, propagating with different phase velocities. The reflection of elastic waves at the solid half-space is investigated using appropriate boundary conditions. The amplitude and energy ratios are calculated based on three different materials, magnesium, titanium, and thallium. It is found that the phase velocities of the propagated elastic waves are functions of linear thermal expansions, thermal relaxation time, thermal conductivity, and specific heat. The phase speed of the elastic waves is found to be high in magnesium as compared to titanium and thallium. We have observed the effect of coefficients of linear thermal expansion numerically on the quasi-thermoelastic wave propagation and the reflection coefficients.

Categories: Materials Engineering, Structural Engineering, Mining Engineering
Keywords: incompressibility, transversely isotropy, thermoelasticity, amplitude ratio, energy ratio

Introduction

Thermoelastic theory is the combination of elastic and heat conduction equations. Biot [1] developed thermodynamical deformation as an irreversible process, he presented the general solutions for thermoelasticity using the Papkovitch-Boussinesq potentials [2]. Lord and Shulman [3] derived the generalized theory of thermoelasticity, which includes a single relaxation time. Norwood and Warren [4] analyzed generalized dynamical theory of thermoelasticity extending the problem to include step-time inputs of strain, temperature, and a stress-free surface. From the study of generalization of classical thermoelasticity, Green and Lindsay [5] obtained simple, explicit expressions for stress tensor, heat conduction vector, and entropy in terms of two scalar functions.

The equations of generalized thermoelasticity for an anisotropic medium were derived by Dhaliwal and Sherief [6], and they obtained the uniqueness equation for an anisotropic medium. Crampin and Taylor [7,8] studied surface wave propagation in multilayered anisotropic medium, and they applied the results numerically in an anistropic medium of zinc oxide, silicon, and sapphire. Verma [9,10] analyzed the dispersion and propagation of elastic waves in fiber-reinforced heat-conducting composite plates modeled as transversely isotropic media. They demonstrated the particle motions for SH modes and are not influenced by thermal variations if the propagation occurs along the axis of symmetry. Banerjee and Pao [11] discussed the phase speeds and attenuation coefficients of the elastic waves in sodium chloride, and they analyzed slowness and thermoelastic surface waves numerically and graphically for NaF and solid helium crystals. Chadwick and Sheet [12] studied quasi-longitudinal, quasi-transverse waves, and pure transverse waves; they obtained numerically the propagation of plane harmonic body waves in a single crystal of zinc. Sharma and Vashishth [13] and Sharma [14] studied intrinsic attenuation and wave propagation in the poroelastic and pre-stressed anisotropic medium, and they analyzed the effect of poroelastic and pre-stressed on the propagation of elastic waves. Keith and Crampin [15] studied seismic body waves in anisotropic media with reflection and refraction, they compared the results with the transversely isotropic medium. Sharma [16] investigated the effect of initial stress on the reflection of plane waves in a general anisotropic medium, and he extended the study to orthotropic materials and explored the existence of specific phase directions. Itskov and Aksel [17] investigated the admissible values of elastic constants for incompressible and compressible anisotropic materials, and they also studied orthotropic and transversely isotropic incompressible as well as isotropically compressible materials. One of the important subclasses of anisotropic medium is transversely isotropy, which is isotropy in the plane perpendicular to the axis of symmetry. Ogden and Singh [18] investigated the effect of rotation and initial stress on surface wave speed in a transversely isotropic medium. The constructive investigation and derivation of basic equations of elastic waves propagating in the general transversely

How to cite this article
Lianngenga R, Lalvohbika J, Lalhriattira F, et al. (May 30, 2025) Effect of Linear Thermal Expansion on Quasi-Thermoelastic Wave in an Incompressible Transversely Isotropy Based on Different Materials. Cureus J Eng 2 : es44388-025-04469-0. DOI https://doi.org/10.7759/s44388-025-04469-0

isotropic medium can be found in Payton [19]. Kerner et al. [20] investigated experimentally the anisotropic clay based on transversely isotropy in the region of South England. The frequency equations of longitudinal and flexural wave propagation in an anisotropic cylinder of transversely isotropic materials were derived by Honarvar et al. [21]. Singh and Goyal [22] studied the propagation of waves in a transversely isotropic microstretch medium, obtaining the reflection and refraction formulas. Chadwick [23] developed the incompressible transversely isotropic elastic body, and he derived the constitutive relations and basic equations. Rouze et al. [24] investigated the elastic wave propagation in transversely isotropic muscle, and they obtained that the phase speed in tissue is greater in magnitude than the normal transversely isotropy. The propagation of elastic waves in non-local transversely incompressible isotropy was studied by Singh [25], and he illustrated wave speed in the particular zinc crystal. Lianngenga and Lalvohbika [26] also discussed the phase speed and reflection coefficients in the transversely isotropy media. Rogerson [27] investigated the dynamic response of an incompressible transversely isotropic elastic body to an impulsive line of force. Ogden and Singh [28] presented the effect of initial stress on the propagation of small amplitude elastic waves in an incompressible transversely isotropic elastic solid.

The propagation of generalized thermoelastic waves in a transversely isotropic medium was studied by Singh and Sharma [29], and they observed that the modified qT-waves were less affected due to thermomechanical coupling effects and thermal relaxation time than the modified qL-waves. Verma and Hasebe [30] obtained the frequency equation of symmetric and antisymmetric modes of vibration in a transversely isotropic thermoelastic plate. Bijarnia and Singh [31] studied the two-dimensional wave propagation in a transversely isotropic thermoelastic solid; they observed the existence of quasi-plane waves. Kumar and Kansal [32] derived the constitutive relations and field equations for anisotropic generalized thermoelastic diffusion and deduced them for a particular type of transverse isotropy; then they investigated Lamb wave propagation in the said medium. Kaur and Plata [33,34] studied Rayleigh and Stoneley wave propagation at the interface of two dissimilar homogeneous transversely isotropic thermoelastic media with two temperatures and rotation. Singh [35] solved the equations of motion and heat conduction equation of an incompressible transversely isotropic thermoelastic solid in view of the Lord and Shulman theory on generalized thermoelasticity, and obtained the secular equation of Rayleigh wave speed for the thermally insulated case and the isothermal case, while the effect of initial stress was discussed by Lalawmpuia and Singh [36] in the transversely isotropic thermoelastic materials.

The change in velocity of seismic waves can be used to determine the structure of the earth's crust [37]. So, the components of velocity and reflection coefficient play an important role in the study of wave propagation in the interior of earth. The reflection of plane waves due to an incident longitudinal wave at a plane free fiber-reinforced thermo-elastic half-space has been investigated by Singh and Zorammuana [38]; they obtained amplitude and energy ratios numerically. The reflection and transmission coefficients of elastic waves were investigated by Lalvohbika and Singh [39] at a corrugated interface between two dissimilar nematic elastomer [39] while the same problems in the incompressible transversely isotropic fiber-reinforced elastic half-spaces were found in [40]. Singh and Tomar [41] obtained amplitude and energy ratios of various reflected waves in thermo-elastic materials with voids and presented graphically for a specific model. Singh and Lianngenga [42] and Singh and Chakraborti [43] investigated the reflection and refraction of elastic waves in the generalized thermoelasticity and micropolar materials respectively, and they presented the results graphically.

This paper dealt with the investigation of incident qP and qT-waves separately in an incompressible transverse isotropic thermoelastic solid half-space. Using Payton [19] and Rouze et al. [25], we obtain the stress-strain relation for incompressible transversely isotropy, and by using Lord and Shulman [3] and Singh [35], we incorporate thermoelastic theory into the stress-strain relation. We observe the existence of two waves, qP and qT, propagating with different phase velocities in this material. The incidence quasi-thermoelastic waves and quasi-secondary waves at an impedance boundary of solid half-space are investigated, and the phase velocities are observed. The amplitude and energy ratios for reflected waves are calculated by considering pressure component of the material. These ratios are functions of the angle of incidence, elastic constants, angular frequency, coefficients of thermal conductivity, increment in temperature, thermal relaxation time, specific heat, and linear thermal expansions. The phase velocities, attenuations, amplitude, and energy ratios of the reflected waves due to incident qP/qT-waves are computed numerically based on transversely isotropic metals: magnesium, titanium, and thallium. The effect of coefficients of linear thermal expansions on these metals is shown graphically using MATLAB software (Table *1*).

Symbols	Expressions
c_{ij}^{*}	Elastic constant
u_j	Displacement component
T	Increment temperature
T_0	Reference temperature
τ_0	Thermal relaxation time
C_e	Specific heat
P	Hydrostatic pressure
ρ	Density
K_i	Coefficient of thermal conductivity
α_i	Coefficient of linear expansion
d_j^{0}	Displacement vector
A & θ	Amplitude constant
v	Phase velocity
A_i	Attenuation
k	Wave number
ω	Frequency
p_j^{0}	Propagation vector
Z_r^{*}	Amplitude ratio
P^{*}	Energy
E_0^{**}	Incident energy ratio
E_r^{**}	Reflected energy ratio
E_r	Energy

TABLE 1: Symbols and their expression

Materials And Methods

Basic equations

Based on the equations of motion and heat conduction equation of generalized thermoelasticity obtained by Lord and Shulman [3], and from Payton [19] and Rouze et al. [25], the incompressible transversely isotropic material is obtained. Then, by combining the two theories we obtain the incompressible transversely isotropic materials in xz -plane, written as [35]

(a) Equation of motion:

$$(c_{11}^{*} u_{1,11})+(c_{13}^{*} + c_{44}^{*}) u_{3,13} + c_{44}^{*}u_{1,33}-\beta_{1}T_{,1} - P_{,1} = \rho \ddot{u}_{1} \tag{1}$$

$$(c_{44}^{*}u_{3,11})+(c_{13}^{*} + c_{44}^{*}) u_{1,13}+c_{33}^{*}u_{3,33}-\beta_{3}T_{,3} - P_{,3} = \rho \ddot{u}_{3} \tag{2}$$

(b) Heat conduction equation:

$$K_1 T_{,11}+K_3 T_{,33} - \rho C_e(\dot{T}+\tau_0\ddot{T})=T_0[\beta_1 (\dot{u}_{1,1} + \tau_0 \ddot{u}_{1,1})+\beta_3 (\dot{u}_{3,3} +\tau_0\ddot{u}_{3,3})] \tag{3}$$

(c) Incompressibility condition:
\begin{equation}\label{sec2.4}
u_{1,1}+u_{3,3}=0-----------(4)
\end{equation}
where $\beta_1 = (c_{11}^* + c_{12}^*)\alpha_1 + c_{13}^*\alpha_3$ and $\beta_3 = 2c_{13}^*\alpha_1 + c_{33}^*\alpha_3$.

Solution of the problem

From Equations (1) and (2), we obtain
\begin{eqnarray}\label{sec3.1}
c_{44}^\ast(u_{1,333}-u_{3,111})+(c_{11}^\ast -c_{13}^\ast -c_{44}^\ast)u_{1,113}+(c_{13}^\ast +c_{44}^\ast -c_{33}^\ast)u_{3,133}\nonumber \\
+(\beta_3 - \beta_1)T_{,13}=\rho(\ddot{u}_{1,3} - \ddot{u}_{3,1})----------(5)
\end{eqnarray}
Consider the solution for Equation (3) and Equation (5) as [36,42]
\begin{eqnarray}\label{sec3.2}
(u_j,T)=(A d_j^0,\theta)\exp\{\imath k(x p_1^0 +z p_3^0-vt)\},~~~~ j=1,3 ----------(6)
\end{eqnarray}
The direction cosine of wave propagation (p_1^0, p_3^0) in xz -plane satisfy
\begin{eqnarray}\label{sec3.3}
(p_1^0)^2 + (p_3^0)^2 =1----------(7)
\end{eqnarray}
Using Equations (6) and (7) into Equations (3) and (5), we obtain
\begin{eqnarray}
(\pi_1 k^2 - \rho \omega^2)A -\pi_2 k \theta &=&0 ----------(8)\label{sec3.4} \\
{\rm and}~~~ \pi_3 k A + (\pi_4 k^2-1)\theta &=& 0 ----------(9)\label{sec3.5}
\end{eqnarray}
where π_i are the coupling parameters, defined as
\begin{equation}
\pi_1=\frac{c_{44}^{*}(d_3^0 (p_1^0)^3-d_1^0 (p_3^0)^3)-(c_{11}^{*}-c_{13}^{*}-c_{44}^{*}) d_1^0 (p_1^0)^2 p_3^0-(c_{13}^{*}+c_{44}^{*}-c_{33}^{*})d_3^0 p_1^0 (p_3^0)^2}{d_3^0 p_1^0-d_1^0 p_3^0}, \nonumber
\end{equation}
\begin{equation}
\pi_2=\frac{(\beta_3-\beta_1)p_1^0 p_3^0}{d_3^0 p_1-d_1^0 p_3^0},\pi_3=\frac{T_0 (\beta_1 d_1^0 p_1^0 + \beta_3 d_3^0 p_3^0)(\omega-\imath\tau_0 \omega^2)}{\rho C_e (\imath\omega+\tau_0 \omega^2)},\pi_4=\frac{K_1(p_1^0)^2 + K_3(p_3^0)^2}{\rho C_e (\imath\omega+\tau_0 \omega^2)} \nonumber
\end{equation}
On solving Equations (8) and (9), we obtain
\begin{eqnarray}
v^2=\frac{a\pm b}{2\rho} ----------(10)\label{sec3.6}
\end{eqnarray}
where $a = B_1$, $b = \sqrt{B_1^2 - 4B_2\rho}$, $B_1 = \pi_1 + \pi_2\pi_3 + \pi_4\rho\omega^2$, $B_2 = \pi_1\pi_4\omega^2$. The Equation (10) is a frequency equation for qP and qT waves bringing all information of the waves propagation.

The root of Equation (10) represents phase velocities for quasi-primary (qP) and quasi-thermal (qT) waves at different propagation vectors. It is noted that $d_1^0 = \cos\theta_0$ and $d_3^0 = -\sin\theta_0$ correspond to qP while $d_1^0 = -\cos\theta_0$ and $d_3^0 = \sin\theta_0$ correspond to qT . It is clear that qP and qT waves are non-homogeneous waves in the dispersive medium.
In the absence of thermal effect ($K_i = T = 0$), we obtain the basic equation previously derived by Kossovich and Moukhomodiarov [44] and phase velocities become [45,46]
\begin{eqnarray}
v^2={\bf a'}/\rho----------(11)
\end{eqnarray}
where $\mathbf{a}' = c_{44}^*\zeta_1^3 - \zeta_2 d_1^0(p_1^0)^2 p_3^0 - \zeta_3 d_3^0 p_1^0 (p_3^0)^2\}/\{d_3^0 p_1^0 - d_1^0 p_3^0\}$, $\zeta_1 = d_3^0(p_1^0)^3 - d_1^0(p_3^0)$, $\zeta_2 = c_{11}^* - c_{13}^* - c_{44}^*$, $\zeta_3 = c_{13}^* + c_{44}^* - c_{33}^*$. The Equation (11) is a frequency equation for qP and qT waves bringing all information of the waves propagation in the absence of thermal effect.

Reflection of waves and boundary conditions

Consider the plane strain parallel to xz -plane with x -axis as horizontal, and the half-space will be $N : \{(x, z) : -\infty < x < \infty, z \leq 0\}$. Mathematically, the boundary conditions at the surface ($z = 0$) can be written as [35]
(i) The normal stress along z - axis vanishes at the surface,
\begin{eqnarray}

t_{33}=-P+(c_{13}^{*}-c_{33}^{*})u_{1,1}-\beta_3 T=0 -----------(12)\label{sec4.1}
\end{eqnarray}
(ii) The tangential stress in xz -plane vanishes,
\begin{eqnarray}
t_{13}=c_{44}^{*}(u_{1,3}+u_{3,1})=0 ----------(13)\label{sec4.2}
\end{eqnarray}
(iii) The displacement component along z-axis is zero,
\begin{eqnarray}
u_1=u_3=0-----------(14)\label{sec4.3}
\end{eqnarray}
Consider the following wave potentials as follows:
\begin{eqnarray}
&& (u_j,T)_{(qP)} = (d_j^0,\eta_0)A_0\exp(\mathcal{P}_0)+\sum_{r=1}^2 (d_j^r,\eta_r) A_r \exp(\mathcal{P}_r), \nonumber \\
&& P_{(qP)} = k_0 F^0A_0 \exp(\mathcal{P}_0)+\sum_{r=1}^2 k_r F^r A_r \exp(\mathcal{P}_r)----------(15)~~\label{sec4.4} \\
&& (u_j,T)_{(qT)} = (d_j^0,\eta_0)A_0\exp(\mathcal{P}_0)+\sum_{r=3}^4 (d_j^r,\eta_r) A_r \exp(\mathcal{P}_r), \nonumber \\
&& P_{(qT)} = k_0 F^0A_0 \exp(\mathcal{P}_0)+\sum_{r=3}^4 k_r F^r A_r \exp(\mathcal{P}_r)----------(16)~~ \label{sec4.5}
\end{eqnarray}
where the 0-superscript and 0-subscript represent incident waves at the surface,

$$\mathcal{P}_0 = \imath k_0(xp_1^0 + zp_3^o - vt) \quad ,\mathcal{P}_r = \imath k_r(xp_1^r + zp_3^r - vt) \quad ,\eta_r = \frac{\pi_3 k_r}{1-\pi_4 k_r^2} \quad ,$$

$$F^r = \frac{1}{\imath}\big[- c_{11}^* d_1^r (p_1^r)^3 - c_{33}^* d_3^r (p_3^r)^3 - (c_{13}^* + 2c_{44}^*) d_3^r (p_1^r)^2 p_3^r$$

$$-(c_{13}^* + 2c_{44}^*) d_1^r p_1^r (p_3^r)^2 - \imath(\beta_1 (p_1^r)^2 + \beta_3 (p_3^r)^2)\frac{\eta_r}{k_r}\big]$$

Note that the values of and p_i^r are obtained from the condition, see Equation (4). Inserting Equations (15)-(16) into given boundary conditions Equations (12)-(14), we have the following system of equations
\begin{eqnarray}
\sum_{r=1}^4 a_{ir}Z_r^\ast &=& a_{i0},~~~\ i=1,2 ----------(17)\label{sec4.6}
\end{eqnarray}
where $r=1,2$ represents incident qP -wave, $r=3,4$ represents incident qT -wave and

$$a_{10} = k_0 F^0 - \imath(c_{13}^* - c_{33}^*) k_0 d_1^0 p_1^0 + \beta_3 \eta_0 \quad ,a_{20} = -\imath c_{44}^*(d_1^0 p_3^0 + d_3^0 p_1^0) k_0 \quad ,$$

$$a_{1r} = -k_r F^r + \imath(c_{13}^* - c_{33}^*) k_r d_1^r p_1^r - \beta_3 \eta_r \quad ,a_{2r} = \imath c_{44}^*(d_1^r p_3^r + d_3^r p_1^r) k_r$$

Solving Equation (17) through Snell's laws, we obtain the following amplitude ratios
\begin{eqnarray}
&& Z_1^*=\frac{a_{10} a_{22}-a_{20} a_{12}}{\phi_1},~~~Z_2^*=\frac{a_{20} a_{11}-a_{10} a_{21}}{\phi_1}, \nonumber \\
&& Z_3^*=\frac{a_{10} a_{24}-a_{20} a_{14}}{\phi_2},~~~Z_4^*=\frac{a_{20} a_{13}-a_{10} a_{23}}{\phi_2} \nonumber
\end{eqnarray}
where $\phi_1 = a_{11}a_{22} - a_{12}a_{21}$ and $\phi_2 = a_{13}a_{24} - a_{14}a_{23}$.

Energy partition

The rate of energy distribution due to incident qP/qT -waves at the surface per unit area is given as [36,38]:
\begin{eqnarray}
P^*=<t_{33}.\dot{u}_3> + <t_{13}.\dot{u}_1> ----------(18)\label{sec5.1}
\end{eqnarray}
Inserting Equations (12)-(16) into Equation (18), the incident energy for coupled qP/qT -waves is given as
\begin{eqnarray}
E_0^{**}=l_0^* \omega k_0 A_0^2 \exp(2\mathcal{P}_0) ----------(19) \label{sec5.2}
\end{eqnarray}
Similarly, the energy due to reflected qP and qT -waves are given by:
\begin{eqnarray}
E_r^{**}=l_r^* \omega k_r A_r^2 \exp(2\mathcal{P}_r) ----------(20)\label{sec5.3}
\end{eqnarray}
where
\begin{eqnarray}
l_0^* &=& \imath[F^0 -\imath(c_{13}^*-c_{33}^*)d_1^0 p_1^0 +\beta_3 \frac{\eta_0}{k_0}] d_3^0 +c_{44}^* [d_1^0 p_3^0 + d_3^0 p_1^0]d_1^0, \nonumber \\
l_r^* &=& \imath[F^r -\imath(c_{13}^*-c_{33}^*)d_1^r p_1^r +\beta_3 \frac{\eta_r}{k_r}] d_3^r +c_{44}^* [d_1^r p_3^r + d_3^r p_1^r]d_1^r \nonumber
\end{eqnarray}

The energy ratio of reflected waves corresponding to incident wave is given as
\begin{equation}
E_r= \frac{l_r^* k_r}{l_0^* k_0} Z_r^{*2}----------(21)
\end{equation}
Note that (E_1, E_2) and (E_3, E_4) are the energy ratios due to incident qP -wave and qT -wave, respectively.

Results

We have derived the formulas for the phase velocities (as shown in Equation 10), the amplitude ratios, and energy ratios for incident qP and qT waves (as shown in Equations 17 and 21) at the surface of an incompressible transversely isotropic solid half-space. These obtained results can be analyzed numerically using the following numerical values for several incompressible transversely isotropic materials (Table 2) such as magnesium, titanium, and thallium [19], and the values of thermal constants are given in Table 3.

Parameter	Magnesium	Titanium	Thallium	Unit
c_{11}^*	0.592×10^{11}	1.62×10^{11}	0.408×10^{11}	Nm^{-2}
c_{12}^*	0.257×10^{11}	0.92×10^{11}	0.354×10^{11}	Nm^{-2}
c_{13}^*	0.214×10^{11}	0.69×10^{11}	0.29×10^{11}	Nm^{-2}
c_{33}^*	0.614×10^{11}	1.81×10^{11}	0.528×10^{11}	Nm^{-2}
c_{44}^*	0.164×10^{11}	0.467×10^{11}	0.0726×10^{11}	Nm^{-2}
ρ	1738	4500	11850	kg/m^3

TABLE 2: Numerical value of elastic constants and density of considered material

Parameter	Value	Unit
K_1	1.24×10^2	$Wm^{-1}degree^{-1}$
K_3	1.34×10^2	$Wm^{-1}degree^{-1}$
C_e	850	$Jkg^{-1}degree^{-1}$
T_0	296	Kelvin
τ_0	0.000001	sec
ω	5	rad/sec
α_1	3.04	K^{-1}
α_3	1.84	K^{-1}

TABLE 3: Value of thermal constants and frequency

Variation of phase velocity at different materials

In this section, Figure 1 represents velocities for qP and qT -waves for considered materials. The corresponding attenuation coefficients are calculated as $\mathcal{A}_r = -Im(\omega/v_r)$, and their values are depicted in Figure 2.
In Figure 1a, velocity $|v_1|$ of the considered materials attains its maximum at $\vartheta_0 = 45^\circ$ and possess the minimum value at normal and grazing angle. In Figure 1b, the value of $|\#v_2|$ gradually decrease as increasing incidence angle (θ_0). From these figures, we see that the velocity of the materials follows the chronological order: magnesium titanium thallium.

In Figure 2a, the attenuation $|\mathcal{A}_1|$ show parabolic curves between normal and grazing incidence angle with maximum values at 45°. In Figure 2b, the attenuation $|\mathcal{A}_2|$ gradually decreases as increasing θ_0. We observe that magnesium exhibits the highest attenuation values while thallium has the least value. It is observed that the velocity and attenuation coefficient of elastic wave propagation achieve highest in magnesium and lowest in thallium, and this result may be useful for manufacturing alloys and electronic devices.

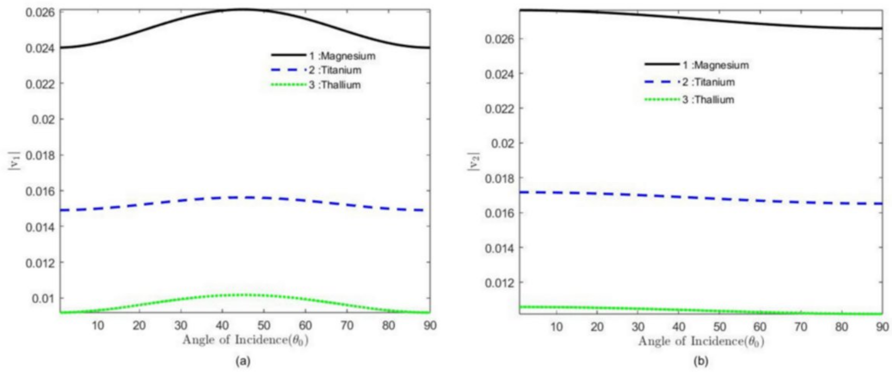

FIGURE 1: Variation of velocities (a) |v1| and (b) |v2| with (qP) angle of incidence

Variation of velocities (a) $|v_1|$ and (b) $|v_2|$ with (qP) angle of incidence

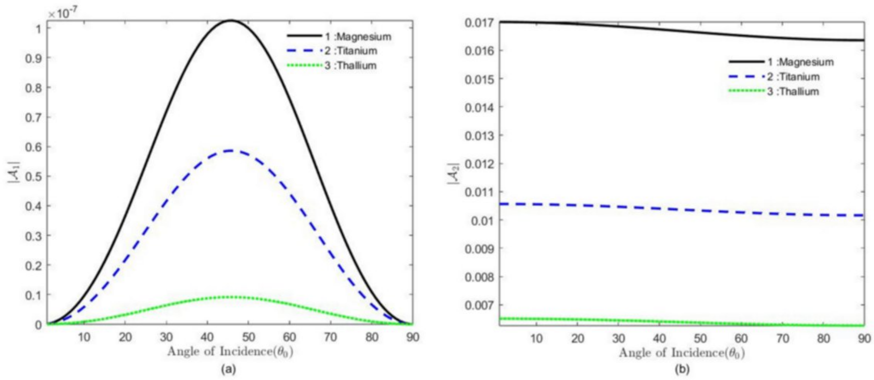

FIGURE 2: Variation of attenuations (a) |A1| and (b) |A2| with |qP| angle of incidence |θ0|

Variation of attenuations (a) $|A_1|$ and (b) $|A_2|$ with |qP| angle of incidence $|\theta_0|$

Effect of thermal expansions on incident qP wave

In this section, Figures 3 to 6 illustrate the variation of amplitude ratios ($|Z_1|$ and $|Z_2|$) and energy ratios ($|E_1|$ and $|E_2|$) against the incident angle (θ_0) for several materials such as magnesium, titanium, and thallium, for the incidence of qP -wave.

In Figure 3, the ratio $|Z_1|$ attains maximum values around $\theta_0 = 44^\circ$, and the minimum values are obtained between $\theta_0 = 50^\circ$ to $\theta_0 = 60^\circ$. We obtain the ranges of $|Z_1|$ is found to be largest in magnesium and smallest in thallium. Magnesium and titanium attain maximum value of $|Z_1|$ at $\alpha_1 = 3.24$ \& $\alpha_3 = 1.64$ while thallium attains at $\alpha_1 = 3.04$ and $\alpha_3 = 1.84$.

In Figure 4, the variation of $|Z_2|$ forms parabolic curves within the intervals 0° to 45° and 45° to 90°. In Figure 4a and b, the maximum value of $|Z_2|$ occur at 36° for magnesium and titanium, while thallium attains the highest value of $|Z_2|$ at 40° when $\alpha_1 = 3.24$ and $\alpha_3 = 1.64$ as shown in Figure 4c. The minimum value of $|Z_2|$ for the considered materials occurs at the normal, grazing and 45° angles of incidence.

Figure 5 illustrate the variation in the energy ratio $|E_1|$, which follows a pattern similar to $|Z_1|$. The effects of linear thermal expansion coefficients on $|E_1|$ are found similar to the ratio $|Z_1|$ as shown in Figure 3.

In Figure 6, the energy ratios $|E_2|$ forms parabolic curves in the region where $|Z_2|$ does in Figure 4. The effect of linear thermal expansions coefficient on $|E_2|$ are more prominent in the range 45° -90° than 0° -45° for considered materials. The maximum value of $|E_2|$ occur at around 50° -60° incident angle.

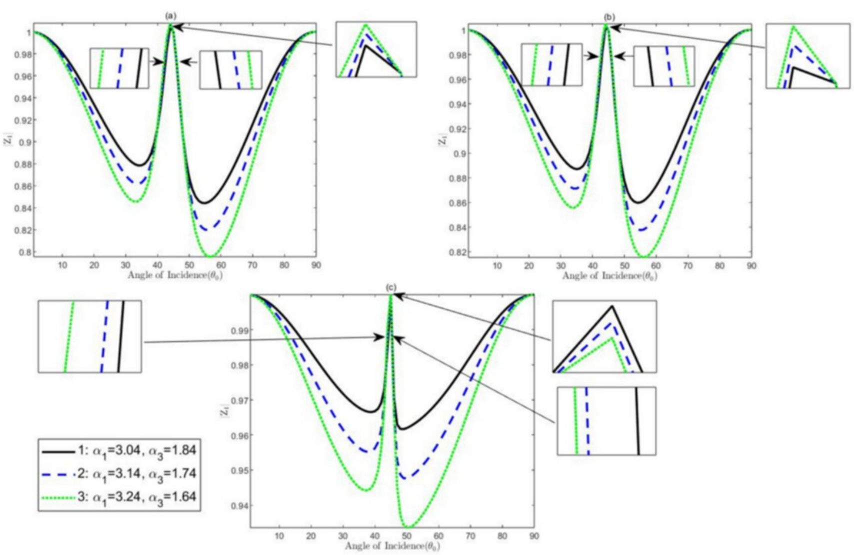

FIGURE 3: Effect of alpha1 and alpha3 on |Z1| of (a) magnesium, (b) titanium, and (c) thallium

Effect of $alpha_1$ and $alpha_3$ on $|Z_1|$ of (a) magnesium, (b) titanium, and (c) thallium

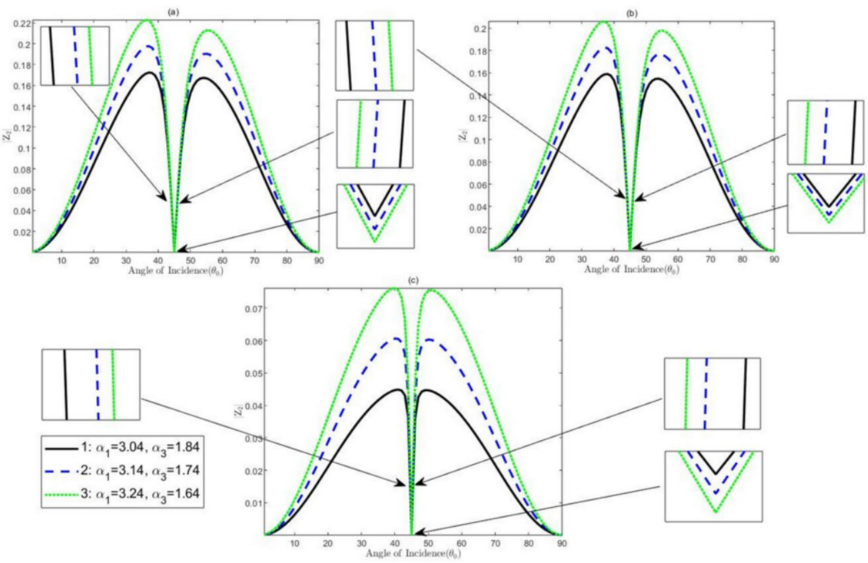

FIGURE 4: Effect of alpha1 and alpha3 on |Z2| of (a) magnesium, (b) titanium, and (c) thallium

Effect of $alpha_1$ and $alpha_3$ on $|Z_2|$ of (a) magnesium, (b) titanium, and (c) thallium

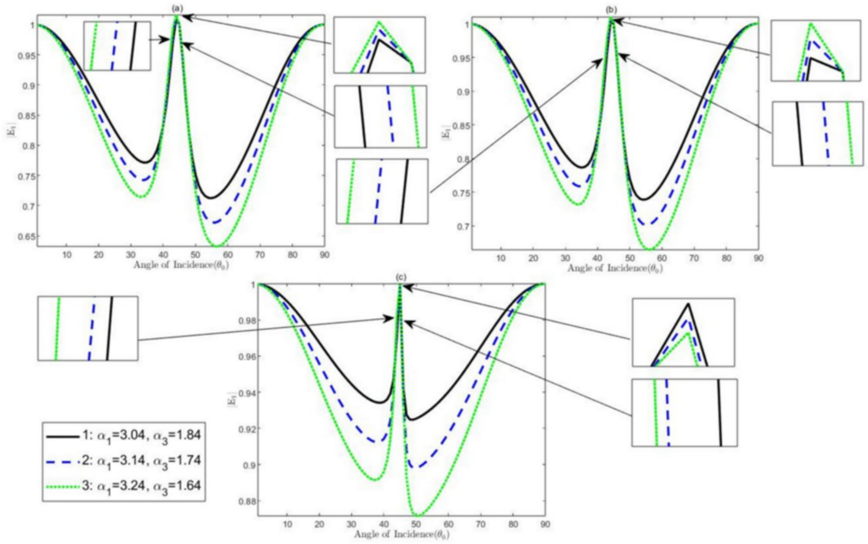

FIGURE 5: Effect of alpha1 and alpha3 on |E1| of (a) magnesium, (b) titanium, and (c) thallium

Effect of alpha$_1$ and alpha$_3$ on |E$_1$| of (a) magnesium, (b) titanium, and (c) thallium

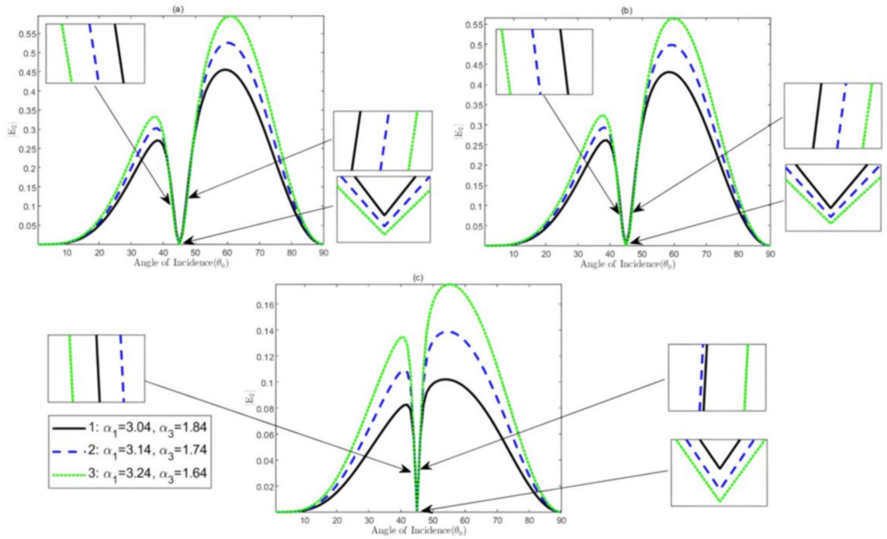

FIGURE 6: Effect of alpha1 and alpha3 on |E2| of (a) magnesium, (b) titanium, and (c) thallium

Effect of alpha$_1$ and alpha$_3$ on |E$_2$| of (a) magnesium, (b) titanium, and (c) thallium

Effect of thermal expansions for incident qT wave

In this section, the variation in amplitude ratios ($|Z_3|$ and $|Z_4|$) and energy ratios ($|E_3|$ and $|E_4|$) for incident qT -wave is expressed and illustrated in Figures 7-10 for magnesium, titanium, and thallium.

In Figure 7, the amplitude ratio $|Z_3|$ exhibits a similar pattern to $|Z_1|$ shown in Figure 3. The maximum and minimum values of $|Z_3|$ occur at 44° and 56°, respectively, when $\alpha_1 = 1.64$ and $\alpha_3 = 3.24$. It is noted that the series of linear thermal expansion effects are in equilibrium at $\theta_0 = 45^\circ$.

In Figure 8, the amplitude ratio $|Z_4|$ has similar pattern to $|Z_2|$ as shown in Figure 4. The maximum value of $|Z_4|$ is found to attain when $\alpha_1 = 1.64$ and $\alpha_3 = 3.24$, while the minimum is found when $\alpha_1 = 1.84$ and $\alpha_3 = 3.04$.

In Figure 9, we observe that the effect of α_1 and α_3 on the energy ratio $|E_3|$ for the considered materials, which are similar to the amplitude ratio $|Z_3|$ as shown in Figure 7.

As shown in Figure 10, the pattern of the energy ratio $|E_4|$ curve resembles the energy ratio $|E_2|$ in Figure 6. The maximum and minimum value of $|E_4|$ for the considered materials occurs when $\alpha_1 = 1.64$ and $\alpha_3 = 3.24$.

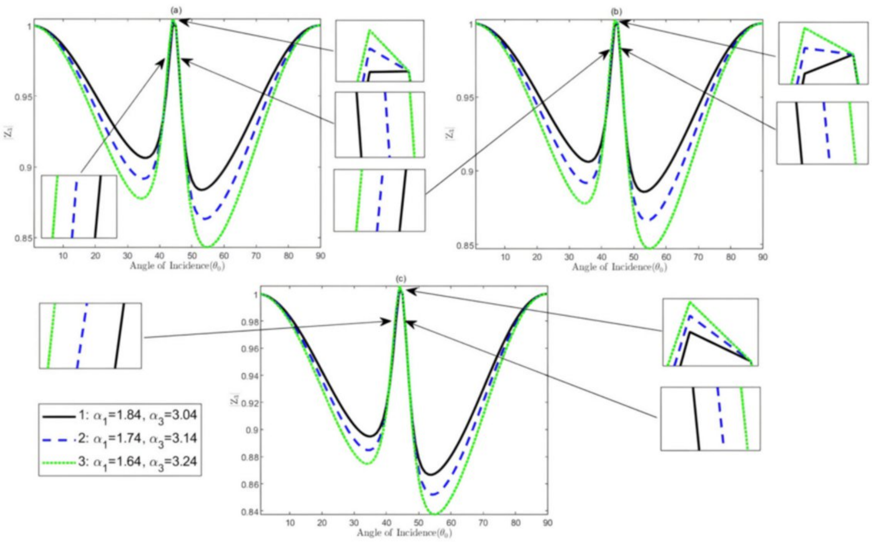

FIGURE 7: Effect of alpha1 and alpha3 on |Z3| of (a) magnesium, (b) titanium, and (c) thallium

Effect of $alpha_1$ and $alpha_3$ on $|Z_3|$ of (a) magnesium, (b) titanium, and (c) thallium

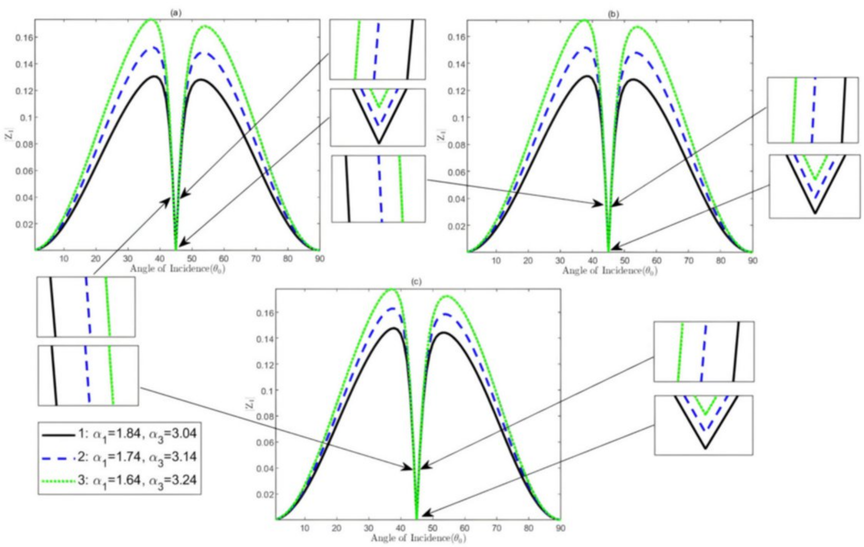

FIGURE 8: Effect of alpha1 and alpha3 on |Z4| of (a) magnesium, (b) titanium, and (c) thallium

Effect of $alpha_1$ and $alpha_3$ on $|Z_4|$ of (a) magnesium, (b) titanium, and (c) thallium

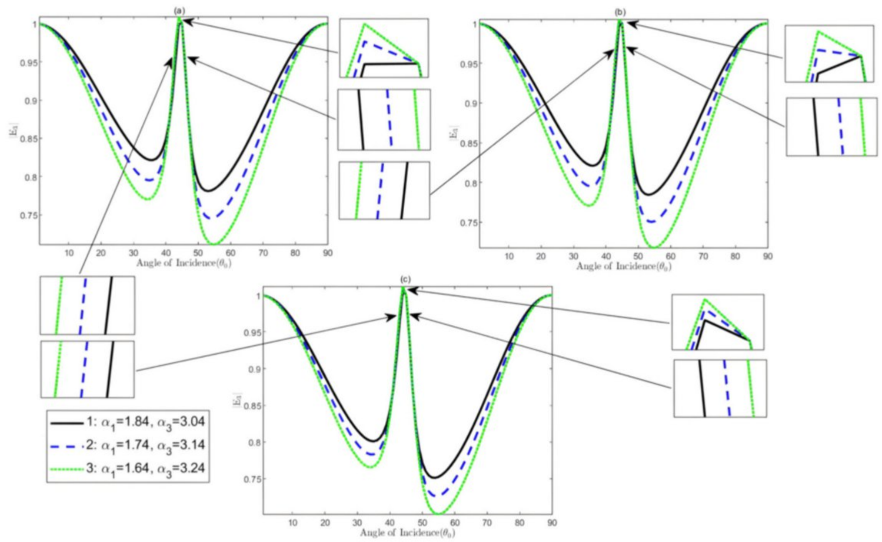

FIGURE 9: Effect of alpha1 and alpha3 on |E3| of (a) magnesium, (b) titanium, and (c) thallium

Effect of alpha$_1$ and alpha$_3$ on $|E_3|$ of (a) magnesium, (b) titanium, and (c) thallium

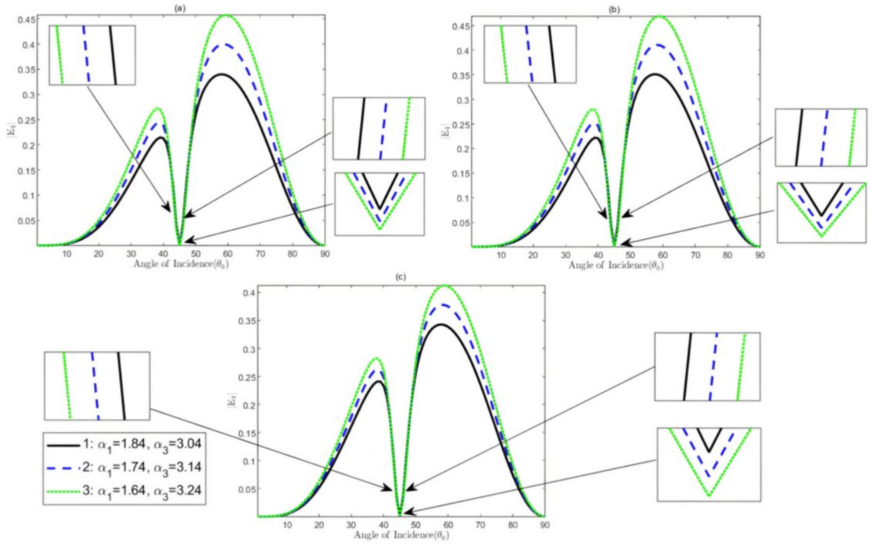

FIGURE 10: Effect of alpha1 and alpha3 on |E4| of (a) magnesium, (b) titanium, and (c) thallium

Effect of alpha$_1$ and alpha$_3$ on $|E_4|$ of (a) magnesium, (b) titanium, and (c) thallium

Discussion

Phase velocity at different materials

As we have seen in Figure *1*, the phase velocities of two body waves $|v_1|$ and $|v_2|$ for different transversely isotropic materials (magnesium, titanium, and thallium) are quite faster than the other anisotropic materials, zinc oxide, silicon, and sapphire, as shown in [7,8]. It is also seen from Verma [9] that the two-phase speeds in the considered materials are slower than the fiber-reinforced heat-conducting composite plate, sodium fluoride [11], the south England clay [20], and transversely isotropic cobalt cylinder [21]. It is found that the low-density material has highest phase speed among the three materials, so it is believed that there must be some essential material properties which may affect the speed of the elastic waves in the considered materials. The phase speed of Rayleigh, Stoneley, and Lamb waves in the homogeneous transversely isotropic thermoelastic media were slower than the speed of qP and qT waves in the considered three different materials [32-34].

The attenuation coefficients $|A_1|$ and $|A_2|$ in the magnesium, thallium, and titanium are smaller than the Dolomite rock [14] while $|A_2|$ in the three different considered materials is larger than the sandstone [13]. The attenuation for the Stoneley waves is much larger than $|A_1|$ and $|A_2|$ of the three considered materials [33]. It is observed that high-density material has low attenuation. This proves that there exists an extra property of the considered materials which may affect the speeds of elastic waves propagating in the three different materials.

Reflected qP waves at different materials

Figures *3* and 4 illustrate $|Z_1|$ and $|Z_2|$ against incident angle (θ_0) for the incidence of qP -wave for magnesium, titanium, and thallium. As shown in Figure *3*, the incident and reflected wave have less difference in the amplitude for all the considered materials, while for the transversely isotropic microstretch materials the reflected waves amplitudes nearly drop to zero at the angle 60° and 45° , as shown in [22]. The similar nature of $|Z_1|$ in the considered materials is also found in generalized micropolar thermoelasticity obtained by Lianngenga and Singh [42] while the smaller corresponding values are found in [39] and [40]. The amplitude ratio $|Z_2|$ in Figure *4* is quite similar to the corresponding ratio in the microstretch materials, with both the reflected waves being smaller than the incident waves [22]. It is also seen that the $|Z_1|$ in Figure *3* is quite similar to the corresponding transversely isotropic materials, while $|Z_2|$ in Figure *4* is very small compared to the corresponding transversely isotropic materials, as seen in [26].

The energy ratios $|E_1|$ and $|E_2|$ in Figures *5* and 6 for the three different materials (magnesium, titanium, and thallium) are larger than the corresponding energy ratios in the transversely isotropic thermoelastic materials, such as cobalt and zinc [36].

Reflected qT wave at different materials

The amplitude ratios $|Z_3|$ and $|Z_4|$ for the incidence of qT -wave for magnesium, titanium, and thallium in Figures *7* and 8 have larger values as compared to the corresponding ratios in the transversely isotropic thermoelastic materials of cobalt and zinc [36] and nematic elastomer [39].

The energy ratios $|E_3|$ and $|E_4|$ in Figures *9* and 10 for the three different materials (magnesium, titanium, and thallium) are quite smaller than the corresponding energy ratios in the transversely isotropic thermoelastic materials of cobalt and zinc [36].

Conclusions

We have analyzed the thermoelastic wave propagating in an incompressible transversely isotropic materials based on the selected materials: magnesium, titanium, and thallium. We obtained the phase velocity, amplitude, and energy ratios for incidence of qP and qT waves. Numerically, the results are expressed graphically to show the effect of linear thermal expansion. The major findings and conclusions are highlighted below:

(i) The phase velocities, amplitude ratios, and energy ratios are functions of angle of incidence, angular frequency, coefficients of thermal conductivity, increment in temperature, thermal relaxation time, specific heat, and linear thermal expansion.
(ii) The parameters, α_1 and α_3 , have no remarkable effect on the phase velocity and their corresponding attenuation.
(iii) The phase velocity of the materials follows the chronological order: magnesium titanium thallium.
(iv) The curves nature of energy ratio $|E_2||$ and $|E_4|$ are similar for incident qP and qT waves.
(v) The amplitude ratio ($|Z_3|$) and energy ratio ($|E_3|$) have equal effect of linear thermal expansion at $\theta_0 = 45^\circ$.
(vi) The amplitude and energy ratios have reverse pattern for incident qP and qT waves.

We have obtained the specific nature of the propagation, amplitude, and energy ratios for magnesium, titanium, and thallium. The knowledge of amplitude and energy ratios helps in understanding the design of sensors and detectors using the considered material plates.

Additional Information

Author Contributions

All authors have reviewed the final version to be published and agreed to be accountable for all aspects of the work.

Concept and design: R. Lianngenga, Jongte Lalvohbika, Fanai Lalhriattira, T.B.C. Laldinnmawia

Drafting of the manuscript: R. Lianngenga, Jongte Lalvohbika, Fanai Lalhriattira, T.B.C. Laldinnmawia

Critical review of the manuscript for important intellectual content: R. Lianngenga, Jongte Lalvohbika, Fanai Lalhriattira, T.B.C. Laldinnmawia

Supervision: R. Lianngenga

Acquisition, analysis, or interpretation of data: Jongte Lalvohbika, Fanai Lalhriattira, T.B.C. Laldinnmawia

Disclosures

Human subjects: All authors have confirmed that this study did not involve human participants or tissue. **Animal subjects:** All authors have confirmed that this study did not involve animal subjects or tissue. **Conflicts of interest:** In compliance with the ICMJE uniform disclosure form, all authors declare the following: **Payment/services info:** All authors have declared that no financial support was received from any organization for the submitted work. **Financial relationships:** All authors have declared that they have no financial relationships at present or within the previous three years with any organizations that might have an interest in the submitted work. **Other relationships:** All authors have declared that there are no other relationships or activities that could appear to have influenced the submitted work.

Acknowledgements

The authors R. Lianngenga and J. Lalvohbika acknowledged the Science and Engineering Research Board (SERB) for the financial assistance through Grant No. CRG/2021/000083 and No. EEQ/2021/000011 to complete this research work.

References

1. Biot MA: Thermoelasticity and irreversible thermodynamics. Journal of Applied Physics. 1956, 27:240-53. 10.1063/1.1722351
2. Benthem JP: Note on the Boussinesq-Papkovich stress-functions. Journal of Elasticity. 1979, 9:201-6. 10.1007/bf00041327
3. Lord H, Shulman H: A generalised dynamical theory of thermoelasticity. Journal of the Mechanics and Physics of Solids. 1967, 15:299-309. 10.1016/0022-5096(67)90024-5
4. Norwood FR, Warren WE: Wave propagation in the generalized dynamical theory of thermoelasticity. The Quarterly Journal of Mechanics and Applied Mathematics. 1969, 22:283-90. 10.1093/QJMAM%2F22.3.283
5. Green AE, Lindsay KA: Thermoelasticity. Journal of Elasticity. 1972, 2:1-7. 10.1007/bf00045689
6. Dhaliwal RS, Sherief HH: Generalized thermoelasticity for anisotropic media. Quarterly of Applied Mathematics. 1980, 38:1-8. 10.1090/qam/575828
7. Crampin S, Taylor DB: The propagation of surface waves in anisotropic media. Geophysical Journal International. 1971, 25:71-87. 10.1111/j.1365-246x.1971.tb02331.x
8. Crampin S, Taylor DB: The dispersion of surface waves in multilayered anisotropic media. Geophysical Journal International. 1970, 21:71-87. 10.1111/j.1365-246X.1970.tb01799.x
9. Verma KL: Thermoelastic slowness surfaces in anisotropic media with thermal relaxation. Latin American Journal of Solids and Structures. 2014, 11:2227-40. 10.1590/s1679-78252014001200006
10. Verma KL: On the propagation of waves in layered anisotropic media in generalized thermoelasticity. International Journal of Engineering Science. 2002, 40:2077-96. 10.1016/s0020-7225(02)00030-7
11. Banerjee DK, Pao YH: Thermoelastic waves in anisotropic solids. The Journal of the Acoustical Society of America. 1974, 56:1444-54. 10.1121/1.1903463
12. Chadwick P, Seet LTC: Wave propagation in a transversely isotropic heat-conducting elastic material. Mathematica. 1970, 17:255-74. 10.1112/S002557930000293X
13. Sharma MD, Vashishth AK: Intrinsic attenuation from inhomogeneous waves in a dissipative anisotropic poroelastic medium. Earth Planets and Space. 2011, 63:89-101. 10.5047/eps.2010.12.004
14. Sharma MD: Wave propagation in a pre-stressed anisotropic generalized thermoelastic medium. Earth Planets and Space. 2010, 62:381-90. 10.5047/eps.2009.12.004
15. Keith CM, Crampin S: Seismic body waves in anisotropic media: reflection and refraction at a plane interface. Geophysical Journal International. 1977, 49:181-208. 10.1111/j.1365-246x.1977.tb03708.x
16. Sharma MD: Existence of transverse waves in anisotropic poroelastic media. Geophysical Journal International. 2008, 174:971-77. 10.1111/j.1365-246x.2008.03855.x
17. Itskov M, Aksel N: Elastic constants and their admissible values for incompressible and slightly compressible anisotropic materials. Acta Mechanica. 2002, 157:81-96. 10.1007/bf01182156
18. Ogden RW, Singh B: Propagation of waves in an incompressible transversely isotropic elastic solid with initial stress: Biot revisited. Journal of Mechanics of Materials and Structures. 2011, 6:453-77. 10.2140/jomms.2011.6.453

19. Payton RG: Elastic Wave Propagation in Transversely Isotropic Media. Martinus Nijhoff Publishers, 1983. 10.1007/978-94-009-6866-0
20. Kerner C, Dyer B, Worthington M: Wave propagation in a vertical transversely isotropic medium: field experiment and model study. Geophysical Journal International. 1989, 97:295-309. 10.1111/j.1365-246x.1989.tb00502.x
21. Honarvar F, Enjilela E, Sinclair AN, Mirnezami SA: Wave propagation in transversely isotropic cylinders. International Journal of Solids and Structures. 2007, 44:5236-46. 10.1016/j.ijsolstr.2006.12.029
22. Singh B, Goyal M: Wave propagation in a transversely isotropic microstretch elastic solid. Mechanics of Advanced Materials and Modern Processes. 2017, 3:8. 10.1186/s40759-017-0023-3
23. Chadwick P: Wave propagation in transversely isotropic elastic media - I. Homogeneous plane waves. Proceedings of the Royal Irish Academy. 1989, 422:23-66. 10.1098/rspa.1989.0019
24. Singh B: Propagation of elastic waves in an incompressible nonlocal transversely isotropic diffusive medium. Acta Mechanica. 2024, 235:4657-68. 10.1007/s00707-024-03968-1
25. Rouze NC, Wang MH, Palmeri ML, Nightingale KR: Finite element modeling of impulsive excitation and shear wave propagation in an incompressible, transversely isotropic medium. Journal of Biomechanics. 2013, 46:2761-68. 10.1016/j.jbiomech.2013.09.008
26. Lianngenga R, Lalvohbika J: Effect of initial stress and impedance boundary in transversely isotropic materials. International Journal of Computational Methods. 2024, 21:2350022. 10.1142/s0219876223500226
27. Rogerson GA: Some dynamic properties of incompressible, transversely isotropic elastic media. Acta Mechanica. 1991, 89:179-86. 10.1007/bf01171254
28. Ogden RW, Singh B: The effect of rotation and initial stress on the propagation of waves in a transversely isotropic elastic solid. Wave Motion. 2014, 51:1108-26. 10.1016/j.wavemoti.2014.05.004
29. Singh H, Sharma JN: Generalized thermoelastic waves in transversely isotropic media. The Journal of the Acoustical Society of America. 1985, 77:1046-53. 10.1121/1.392391
30. Verma KL, Hasebe N: Wave propagation in transversely isotropic plates in generalized thermoelasticity. Archive of Applied Mechanics. 2002, 72:470-82. 10.1007/s00419-002-0215-z
31. Bijarnia R, Singh B: Propagation of plane waves in an anisotropic generalized thermoelastic solid with diffusion. Journal of Engineering Physics and Thermophysics. 2012, 85:478-86. 10.1007/s10891-012-0676-z
32. Kumar R, Kansal T: Propagation of Lamb waves in transversely isotropic thermoelastic diffusive plate. International Journal of Solids and Structures. 2008, 45:5890-913. 10.1016/j.ijsolstr.2008.07.005
33. Kaur I, Lata P: Stoneley wave propagation in transversely isotropic thermoelastic medium with two temperature and rotation. GEM - International Journal on Geomathematics. 2020, 11:4. 10.1007/s13137-020-0140-8
34. Kaur I, Lata P: Rayleigh wave propagation in transversely isotropic magneto-thermoelastic medium with three-phase-lag heat transfer and diffusion. International Journal of Mechanical and Materials Engineering. 2019, 14:12. 10.1186/s40712-019-0108-3
35. Singh B: Wave propagation in an incompressible transversely isotropic thermoelastic solid. Meccanica. 2015, 50:1817-25. 10.1007/s11012-015-0126-z
36. Tochhawng L, Singh SS: Effect of initial stresses on the elastic waves in transversely isotropic thermoelastic materials. Engineering Reports. 2020, 2:e12104. 10.1002/eng2.12104
37. Christensen NI, Mooney WD: Seismic velocity structure and composition of the continental crust: a global view. Journal of Geophysical Research. 1995, 100:9761-88. 10.1029/95jb00259
38. Singh SS, Zorammuana C: Incident longitudinal wave at a fibre-reinforced thermoelastic half-space. Journal of Vibration and Control. 2013, 20:1895-906. 10.1177/1077546313483785
39. Lalvohbika J, Singh SS: Effect of corrugation on incident qP/qSV-waves between two dissimilar nematic elastomers. Acta Mechanica. 2019, 230:3317-38. 10.1007/s00707-019-02458-z
40. Lalvohbika J, Singh SS: Waves due to corrugated interface in incompressible transversely isotropic fiber-reinforced elastic half-spaces. Mechanics of Advanced Materials and Structures. 2020, 29:1720-29. 10.1080/15376494.2020.1838005
41. Singh J, Tomar SK: Plane waves in thermo-elastic material with voids. Mechanics of Materials. 2007, 39:932-40. 10.1016/j.mechmat.2007.03.007
42. Lianngenga R, Singh SS: Reflection of coupled dilatational and shear waves in the generalized micropolar thermoelastic materials. Journal of Vibration and Control. 2020, 26:1948-55. 10.1177/1077546320908705
43. Singh MC, Chakraborty N: Reflection and refraction of P-, SV- and thermal wave, at an initially stressed solid-liquid interface in generalized thermoelasticity. Applied Mathematical Modelling. 2013, 37:463-75. 10.1016/j.apm.2012.03.008
44. Kossovich LY, Moukhomodiarov RR, Rogerson GA: Analysis of the dispersion relation for an incompressible transversely isotropic elastic plate. Acta Mechanica. 2002, 153:89-111. 10.1007/bf01177053
45. Singh B: Wave propagation in an initially stressed transversely isotropic thermoelastic solid half-space. Applied Mathematics and Computation. 2010, 217:705-15. 10.1016/j.amc.2010.06.008
46. Singh B: Wave propagation in an incompressible transversely isotropic fibre-reinforced elastic media. Archive of Applied Mechanics. 2007, 77:253-58. 10.1007/s00419-006-0094-9